

## GaInNAs/GaAs quantum wells grown by molecular-beam epitaxy emitting above 1.5 $\mu\text{m}$

E. Tournié,<sup>a)</sup> M.-A. Pinault, and M. Laügt

Centre de Recherche sur l'Hétéro-Epitaxie et ses Applications, Centre National de la Recherche Scientifique (CRHEA/CNRS), Rue Bernard Grégory, Parc Sophia Antipolis, F-06560 Valbonne, France

J.-M. Chauveau, A. Trampert, and K. H. Ploog

Paul-Drude-Institut für Festkörperelektronik Hausvogteiplatz 5-7, D-10117 Berlin, Germany

(Received 15 November 2002; accepted 28 January 2003)

We demonstrate that a careful optimization of the molecular-beam-epitaxy growth conditions allows us to obtain high-quality GaInNAs/GaAs quantum-well (QW) heterostructures exhibiting a perfect two-dimensional microstructure at high In and N contents. Room-temperature emission is achieved up to 1.61 and 1.51  $\mu\text{m}$  for as-grown and annealed samples, respectively. High-resolution x-ray diffraction and transmission electron microscopy reveal that post-growth annealing does not affect the QW composition and width. This confirms that the GaInNAs semiconducting material is well suited for emission in the telecommunication wavelength range near 1.55  $\mu\text{m}$ . © 2003 American Institute of Physics. [DOI: 10.1063/1.1563062]

Long-wavelength lasers emitting in the 1.3-to-1.6- $\mu\text{m}$  range form the cornerstone of telecommunications optoelectronic devices. Most devices up to now have relied on InP-based semiconductor heterostructures. Recently, much work has been focused on the development of a new family of GaAs-based compounds, namely, the GaInNAs (GINA) semiconducting alloys, which appear as a promising alternative for these applications.<sup>1</sup> Indeed, impressive results have been obtained with edge-emitting<sup>2</sup> as well as vertical-cavity surface-emitting lasers<sup>3-5</sup> operating near 1.3  $\mu\text{m}$ . Still, the possibility to obtain an emission at 1.5  $\mu\text{m}$  or even longer wavelengths remains very elusive. Even though laser emission has been reported at 1.52  $\mu\text{m}$  with the GINA/GaAs materials system,<sup>6</sup> and we have observed low-temperature photoluminescence (PL) up to 1.7  $\mu\text{m}$ ,<sup>7</sup> it is often suggested that this materials system is not appropriate to reach the 1.5- $\mu\text{m}$ -wavelength range at room temperature, and that other systems should be used.<sup>8-10</sup> In fact, RT PL around 1.5  $\mu\text{m}$  has been demonstrated from GaAsSbN/GaAs quantum wells (QWs),<sup>8</sup> GaInNAsSb/GaNAsSb QWs<sup>9</sup> or GINA/GaAs quantum dots.<sup>10</sup> In this letter, we show that RT PL can indeed be achieved up to 1.6  $\mu\text{m}$  with GINA/GaAs QWs exhibiting a perfect two-dimensional (2D) morphology.

The samples were grown on (001) GaAs substrates in a Riber system equipped with conventional solid sources for group-III and As elements, and with an Addon rf plasma source for N. For each sample, a GaAs buffer layer was first grown at  $\sim 580^\circ\text{C}$ . The sample temperature was then decreased down to 400–420  $^\circ\text{C}$  for growing the  $\text{Ga}_{1-x}\text{In}_x\text{N}_y\text{As}_{1-y}$  QW and about 10 monolayers (ML) GaAs. The remaining GaAs top barrier layer (65 nm) was then grown at  $\sim 580^\circ\text{C}$ . Finally, all samples were capped with an AlGaAs window layer. Growth runs were controlled by *in situ* reflection high-energy electron diffraction (RHEED). *Ex situ* annealing of all samples has been performed in a conventional furnace under a flowing- $\text{N}_2$  ambi-

ent with GaAs proximity capping. The samples were annealed for 1 h at 680  $^\circ\text{C}$ , which correspond to the optimum conditions in this setup in terms of PL properties of GINA QWs. As-grown samples have been investigated by temperature-dependent PL spectroscopy, using the 488-nm line of an Ar laser and a cooled Ge detector. Some samples were investigated by transmission electron microscopy (TEM) and high-resolution x-ray diffraction (HRXRD).

GINA-based heterostructures designed for emission at 1.3  $\mu\text{m}$  rely on  $\sim 7$ -nm-wide QWs with In and N contents around 35% and  $\sim 1\%$ , respectively.<sup>1-5</sup> To reach longer wavelengths, one should adjust these three parameters. However, since N has the strongest effect on the band gap,<sup>1</sup> we have chosen to increase essentially the N content and the QW width. We show in Fig. 1 the evolution of the intensity of the RHEED specular spot recorded during growth of the GaAs buffer layer and of the GINA QW for a typical sample. Very clear oscillations are observed throughout the whole QW growth, which reveals a perfect bidimensional growth mode and the absence of any phase separation, which is a

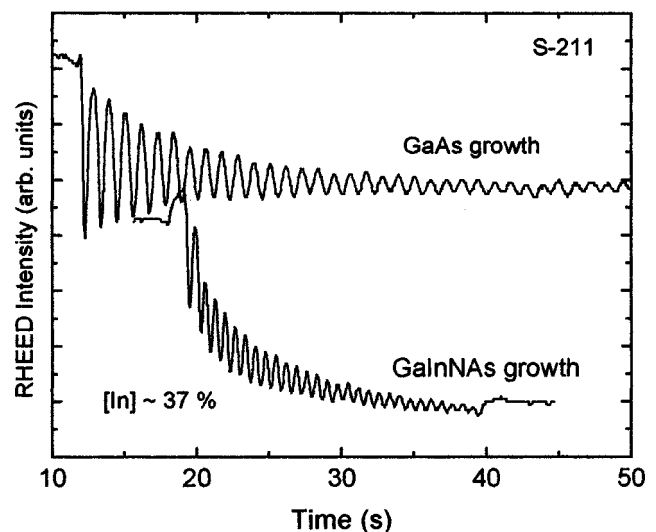


FIG. 1. RHEED intensity oscillations recorded during growth of the GaAs buffer layer and of the GINA QW.

<sup>a)</sup>Present address: Université Montpellier II, CEM2—UMR CNRS 5507, CC 067, F-34095 Montpellier cedex 5; electronic mail: etournie@univ-montp2.fr

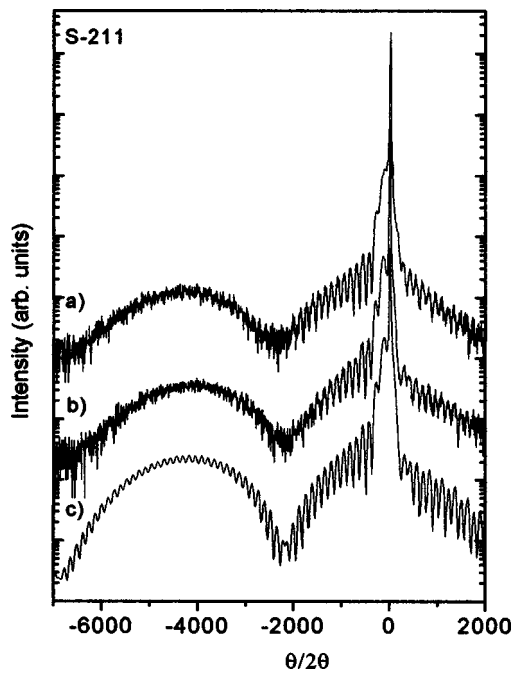


FIG. 2. HRXRD rocking curves obtained from sample S-211: as-grown sample (a), annealed sample (b), and simulated pattern (c). The curves have been vertically shifted for clarity.

crucial criterion in view of achieving high PL efficiency.<sup>11</sup> Finally, we can directly extract an In content of 37% and a QW width of 29 ML.

Figure 2 displays the HRXRD pattern taken from the as-grown sample (a), from the same sample after *ex situ* annealing (b), together with the simulated rocking curve (c). Best fit is obtained assuming 35% In (which lies within the

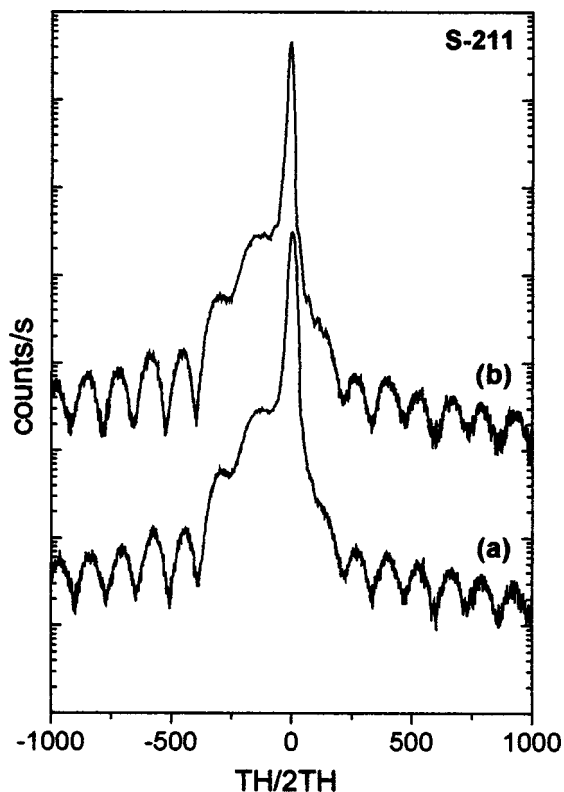


FIG. 3. Details of the HRXRD rocking curves obtained from the as-grown (a) and annealed (b) sample S-211. The curves have been vertically shifted for clarity.

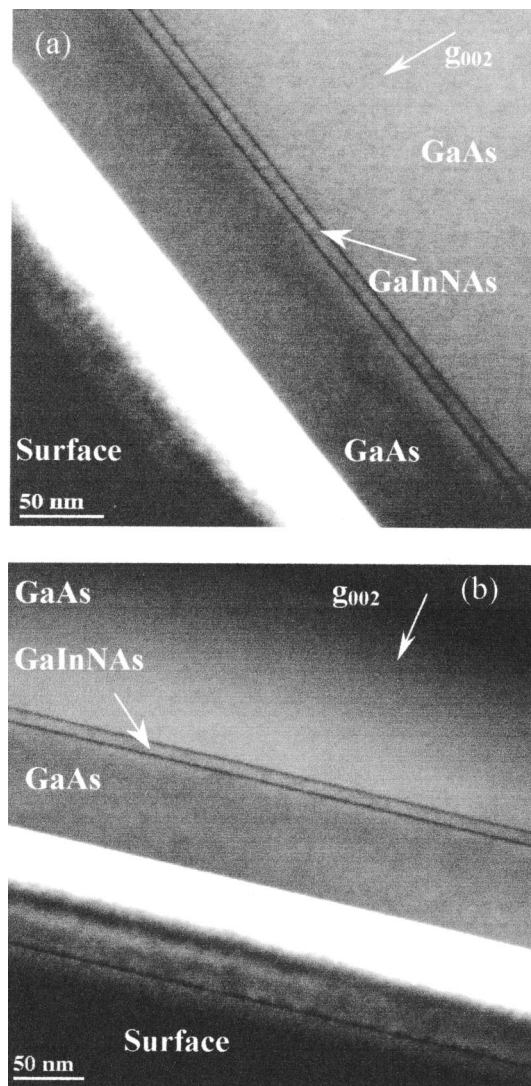


FIG. 4. (110) cross-sectional dark-field TEM images using the diffraction vector  $\mathbf{g}=002$  for (a) as-grown and (b) annealed sample S-211.

error bar of the RHEED measurements) and 3.6% N in the QW. The striking point is the perfect agreement observed between all three curves. This demonstrates unambiguously that the QW composition and width remain unchanged after annealing. This confirms that the influence of annealing on the properties of GINA based heterostructures is to be searched for inside the QW itself, and does not arise from any out- or interdiffusion of any element at the QW interfaces.<sup>12</sup>

The details of the rocking curves in the vicinity of the main diffraction peak are given in Fig. 3. One can verify that even on this scale, there is a perfect agreement between the rocking curves taken from annealed and as-grown samples. However, a careful inspection of this figure reveals a significant narrowing of the width of the diffraction peak, together with an enhanced peak-to-valley contrast for the Pendellösung fringes (Fig. 3). This shows that post-growth annealing induces a noticeable improvement of the overall crystalline quality of the heterostructure.

Next, Figs. 4(a) and 4(b) show the cross-sectional TEM images from sample S-211 taken with a diffraction vector  $\mathbf{g}=002$ . Under these conditions, the observed contrasts are related to the chemical composition of the alloy. The combi-

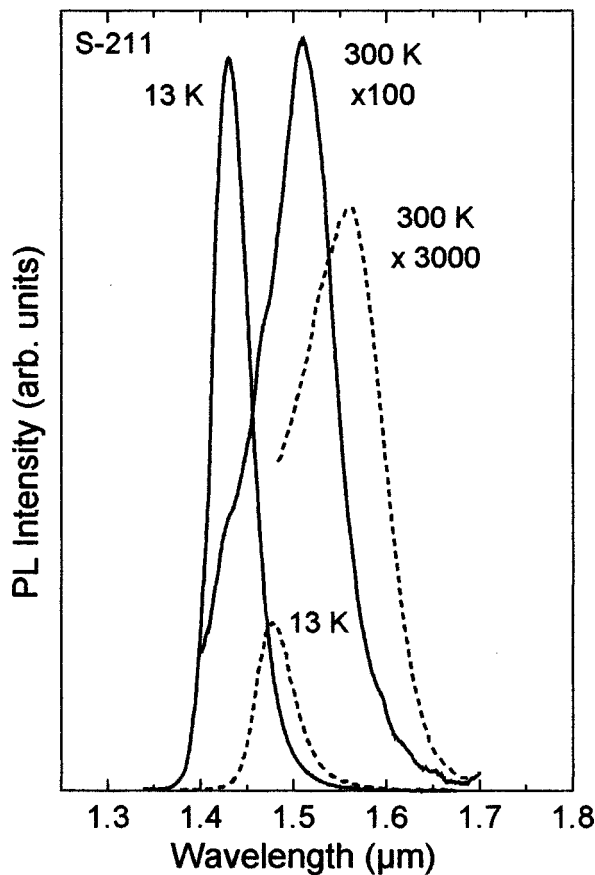


FIG. 5. PL spectra taken from as-grown (dashed line) and annealed (solid line) sample S-211.

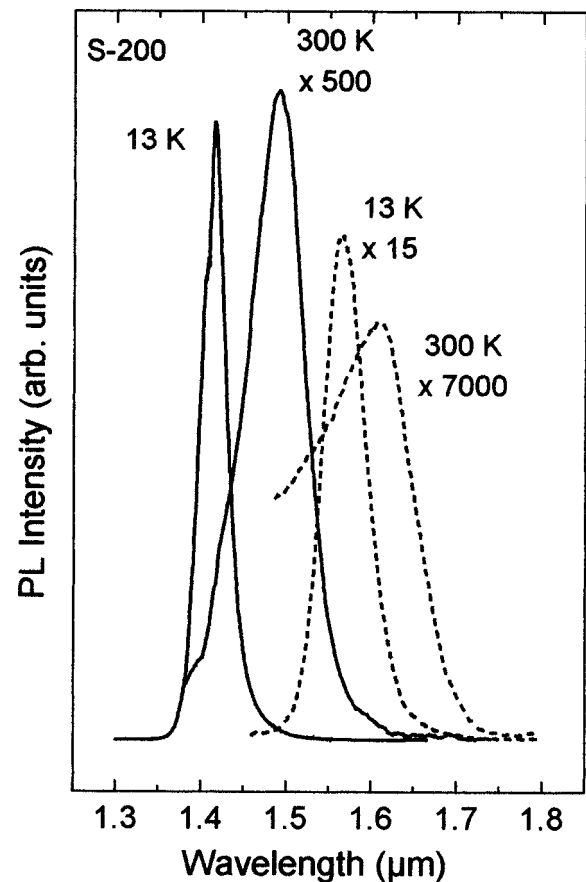


FIG. 6. PL spectra taken from as-grown (dashed line) and annealed (solid line) sample S-200.

nation with local strain measurements extracted from high-resolution TEM images furthermore allows is to determine the composition of the quaternary GINA QW.<sup>13,14</sup> Based on this method, we have calculated In compositions of 35.5% and 36%, and N contents of 3.6% and 3.2%, before and after annealing, respectively. These values are identical within the experimental error determined by the procedure given in Ref. 14. Therefore, no evidence for a compositional change in the QWs is found as a result of out-diffusion. In fact, the TEM micrographs also demonstrate no significant evolutions of the QW width after the heat treatment: 9.2 nm and 9.6 nm before and after annealing, respectively. As seen in Fig. 4(a), the as-grown QW already exhibits a perfect 2D morphology, even at such high N content. Furthermore, within our detection limit, there is no indication for lateral composition fluctuations along the QW as it is observed, for instance, in Ref. 14. Therefore, we can conclude that the variations in the structure and/or composition of our GINA QWs after annealing must occur on a smaller length scale.

Finally we show in Figs. 5 and 6 the PL spectra taken from the two samples the structural properties of which have been presented earlier. Sample S-211 peaks at 1.56  $\mu\text{m}$ , while sample S-200 peaks at as long a wavelength as 1.61  $\mu\text{m}$  at room temperature. To our knowledge, this is the longest wavelength reported so far with this materials system. After annealing, the radiative efficiency is strongly enhanced and is comparable to or higher than that of N-free GaInAs parent QWs. Although the PL line is blueshifted, as is usual for GINA QWs,<sup>12</sup> emission above 1.5  $\mu\text{m}$  is observed.

Our results thus show that a careful adjustment of the growth conditions allows vs to obtain GINA/GaAs heterostructures with a high structural perfection that emit above 1.5  $\mu\text{m}$ .

Part of this work was sponsored by the FET arm of the IST program of the European Commission (project IST-2000-26478-GINA1.5).

<sup>1</sup>E. Tournié and B. Gil, in *Low Dimensional Particle Semiconductors*, edited by B. Gil (Oxford, London, 2002), p. 415–455.

<sup>2</sup>S. Illek, A. Ultsch, B. Borchert, A. Y. Egorov, and H. Riechert, *Electron. Lett.* **36**, 725 (2000).

<sup>3</sup>C. W. Coldren, M. C. Larson, S. G. Spruytte, and J. S. Harris, *Electron. Lett.* **36**, 951 (2000).

<sup>4</sup>G. Steinle, H. Riechert, and A. Y. Egorov, *Electron. Lett.* **31**, 93 (2001).

<sup>5</sup>A. Ramakrishnan, G. Steinle, D. Supper, C. Degen, and G. Ebbinghaus, *Electron. Lett.* **38**, 322 (2002).

<sup>6</sup>M. Fischer, M. Reinhardt, and A. Forchel, *Electron. Lett.* **36**, 1208 (2000).

<sup>7</sup>E. Tournié, M. A. Pinault, S. Veziar, J. Massies, and O. Tottereau, *Appl. Phys. Lett.* **77**, 2189 (2000).

<sup>8</sup>G. Ungaro, G. Le Roux, R. Teissier, and J. C. Harmand, *Electron. Lett.* **35**, 1246 (1999).

<sup>9</sup>W. Ha, V. Gambin, M. Wistey, S. Bank, H. Yuen, S. Kim, and J. S. Harris, *Electron. Lett.* **38**, 277 (2002).

<sup>10</sup>M. Sopanen, H. P. Xin, and C. W. Tu, *Appl. Phys. Lett.* **76**, 994 (2000).

<sup>11</sup>M. A. Pinault and E. Tournié, *Appl. Phys. Lett.* **79**, 3404 (2001).

<sup>12</sup>E. Tournié, M. A. Pinault, and A. Guzman, *Appl. Phys. Lett.* **80**, 4148 (2002).

<sup>13</sup>J. M. Chauveau, A. Trampert, K. H. Ploog, M.-A. Pinault, and E. Tournié, *J. Cryst. Growth* (in press).

<sup>14</sup>V. Grillo, M. Albrecht, T. Remmele, H. P. Strunk, A. Yu. Egorov, and H. Riechert, *J. Appl. Phys.* **90**, 3792 (2001).